IEEE Access
Multidisciplinary : Rapid Review : Open Access Journal

Received January 12, 2021, accepted February 12, 2021, date of publication February 22, 2021, date of current version March 9, 2021.

Digital Object Identifier 10.1109/ACCESS.2021.3061263

An Improved Inertial Matching Algorithm for Hull Deformation With Large Misalignment Angle

DONGSHENG XU[1], XIAFU PENG[1], XIAOLI ZHANG[1], GONGLIU YANG[2], AND XIAOQIANG HU[1]

[1]Department of Automation, School of Aeronautics and Astronautics, Xiamen University, Xiamen 361005, China
[2]School of Instrumentation and Optoelectronic Engineering, Beihang University, Beijing 100191, China

Corresponding author: Xiafu Peng (xfpeng@xmu.edu.cn)

This work was supported in part by the Fundamental Research Funds for the Central Universities under Grant 20720190129, in part by the Industry-University Cooperation Project (IUCP) of Fujian Province under Grant 2017H6101, and in part by the National Natural Science Foundation of China under Grant 61703356.

ABSTRACT Inertial matching measurement method has been widely used to measure hull deformation in real time to establish a unified attitude reference for ships in previous decades, but most current methods were based on linear error model which adopted small angle approximation. Therefore, the large misalignment angle in the hull deformation will bring great challenges to the accuracy of inertial matching measurement methods. In order to solve this problem, we divided the hull deformation with large misalignment angle into two parts: large angle based on coarse registration and small angle of the residual part. Three improvements were made as the following: (1) The quaternion optimization method (Q) was utilized to get the coarse registration result; (2) Based on the result, we derived a brand-new residual small-angle measurement algorithm. (3) We introduced neural network Karman filter (NNKF) to calculate the hull deformation in real time to further reduce the nonlinear error of the system. The experiment results illustrated that the proposed method, namely, Q-NNKF, can accurately measure the hull deformation in real time and effectively suppressed the nonlinear error caused by large misalignment angle.

INDEX TERMS Inertial matching measurement, hull deformation algorithm, large misalignment angle, neural network Kalman filter.

I. INTRODUCTION

Inertial navigation system provides the position parameters, attitude parameters and motion parameters of the carrier by measuring the acceleration and angular velocity of the carrier with gyroscope and accelerometer respectively. The fiber optic gyroscope strapdown inertial measurement unit (FGU) has the distinct advantages such as simple structure, small volume, low cost and simple maintenance, which can be fixedly connected to the carrier to provide digital navigation information, [1], [2]. Inertial navigation system can obtain navigation information without external information, thus modern ships such as aircraft carriers, ocean-going destroyers, astronautic measurement ship, and so on, usually need to navigate with the help of high-precision inertial navigation system or platform compass [3]–[5]. In order to ensure the normal operation of radar, missile launcher, phalanx close and other shipborne equipment, we need to provide a unified attitude reference for shipboard equipment. We provide accurate navigation parameters to the navigation system of shipborne equipment to complete the binding of the initial navigation parameters so as to adjust them quickly into the accurate working state, and this process is referred to as a transfer alignment [6]–[8]. However, the ship is not a rigid body. With the change of the load of ship, the impact of sea waves and other external forces, as well as the internal structure changes of the ship caused by the long-term effect of expansion and contraction with temperature, the ship will undergo hull deformation, forming a certain misalignment angle between the main inertial navigation system and shipboard equipment, which we call hull deformation. Due to the existence of hull deformation, ship-borne equipment directly using navigation parameters provided by the central inertial navigation system will bring misalignment angle error, resulting in the lack of accuracy. Therefore, the measurement of hull deformation is fast becoming a key instrument in improving navigation accuracy.

A.V. Mochalov *et al.* found that the hull deformation angle can be as high as 1° to 1.5° [9]. In order to overcome the effect of hull deformation and establish a unified

The associate editor coordinating the review of this manuscript and approving it for publication was Pietro Savazzi.

navigation coordinate datum for the whole ship, scholars all over the world have adopted structural mechanics methods such as oversize steel tube datum method, dual-source CCD measurement method, photogrammetry method and grating method to measure hull deformation. However, these methods often have shortcomings, including insufficient accuracy, poor implementability, and inability to obtain the linear velocity change of dynamic deformation angle in real time. The Central Institute of Electrical Instruments and the Institute of Electrical Engineering in St. Petersburg, Russia, put forward the method of measuring hull deformation by inertial measurement matching method in the late 1980s. By using the difference of navigation information between inertial measurement components installed on shipboard equipment and the high-precision main inertial navigation, the deviation caused by deformation angle can be detected and corrected in real time by Kalman filter [9]. Inertial measurement of hull deformation has the advantages of no dependence on external equipment, easy installation and good real-time performance, so it has become the most promising research direction in current deformation measurement. The long-term static deformation angle of hull is usually modeled as a constant or random walk process, and the dynamic deformation is usually modeled as a second-order Markov model [10]–[12]. Inertial matching method of hull deformation measurement can be calculated by using various navigation information, such as angular velocity matching, attitude matrix matching, velocity and angular velocity combination matching, etc. These algorithms are based on linear model, which means that the algorithm can only operate when the misalignment angle of hull deformation is small.

In the long-term voyage of ships, due to the limitation of installation conditions and the aging of the hull deck in the harsh external environment, the misalignment angle of hull deformation will further increase, resulting in the calculation error of the conventional inertia matching algorithm of hull deformation increasing or even diverging [15]. Therefore, matching algorithm of hull deformation under large misalignment angle has been a largely under explored domain. In view of the nonlinear problem caused by large misalignment angle, the paper [13] put forward the idea of roughly estimating large misalignment angle. Huang Yulong *et al.* completed Kalman filtering for coarse alignment of motion by using odometer assisted Strapdown Inertial Navigation System [14]. The paper [15] proposed a solution to transform the alignment problem into quaternion optimization problem, which provides a reference for reducing the nonlinear error of hull deformation under large misalignment angle. In the process of inertial matching of hull deformation, we need Kalman filter for accurate calculation [16]–[18]. Under large misalignment angle, conventional Kalman filter is associated with increased risk of error increase or divergence, so we need adaptive Kalman filter to deal with nonlinear problem [19], [20]. Ying He *et al.* put forward the guiding ideology of combining neural network with Kalman filter [21]. Nevertheless, the algorithm for hull deformation with large arbitrary installation misalignment angle still need to be solved urgently.

In order to solve the above problems, we introduced an improved inertial matching algorithm, namely, Q-NNKF, for the hull deformation with large misalignment angle. In this paper, we divided the hull deformation into two parts: the large angle obtained by coarse registration and the small residual angle. (1) We used the quaternion optimization method to rapidly get the coarse registration result of large misalignment angle quickly; (2) Using the result, we derive a brand-new small-angle residual measurement equation to reduce the nonlinearity of the system. (3) In order to ensure the accuracy of the algorithm and further reduce the nonlinear error of the system, the NNKF was utilized to calculate the hull deformation in real time. Finally, semi-physical simulation platform tests are carried out to verify the validity and applicability of the investigated method.

The rest of the content is organized as follows. Section II presents the reference frame definitions. Section III introduces the Q-NNKF algorithmincluding the derivation of quaternion optimization method, a new attitude matching algorithm and the neural network Karman filter. Section IV we narrated our hardware work for experimental platform construction and conducted many experiments to compare the proposed method and existing hull deformation algorithm. The conclusions are given in Section V.

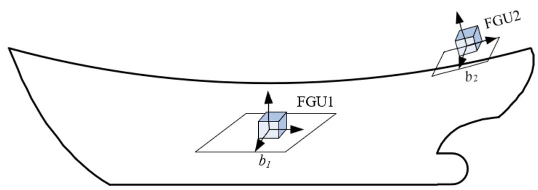

FIGURE 1. FGUs installation in deformation measurement on the ship.

II. THE REFERENCE FRAME DEFINITIONS

In hull deformation measurement, FGUs are respective installed near the shipboard equipment and the main navigation system, which are named as FGU1 and FGU2 as shown in Figure 1. Because the hull is not a rigid body, there will be a changing misalignment angle φ_{12} between FGU1 coordinate system b_1 and FGU2 coordinate system b_2, which is the hull deformation angle. When the hull deformation φ_{12} is a large misalignment angle, the scheme proposed in this paper divides the hull deformation φ_{12} into two parts: φ_{10} and φ_{02}. φ_{02} is the large angle calculated by coarse registration, and φ_{10} is the residual part of hull deformation angle.

The coordinate frames mentioned in this paper are defined as follows:

(1) b_1, b_2: Carrier coordinate system corresponding to FGU1 and FGU2 installation position, respectively.

(2) b_0: The coordinate system which have the angle φ_{02} with b_2.

(3) i_1, i_2: The body coordinate systems of FGU1 and FGU2 at the initial time t_0 which remain stationary in the inertial space, relatively.

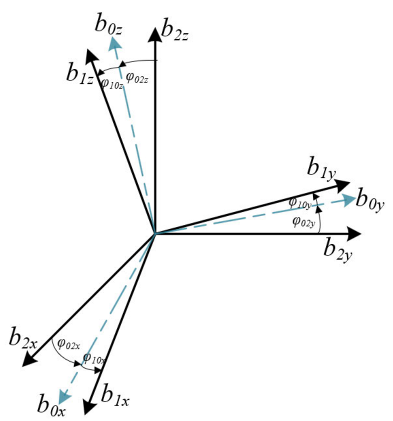

FIGURE 2. Three-dimensional coordinate definition of FGU1 and FGU2.

(4) i_0: The coordinate system of b_0 at the initial time t_0 which remain stationary in the inertial space.

(5) $\tilde{i}_1$, $\tilde{i}_2$: The coordinate systems respectively coincided with i_1 and i_2 at the initial time t_0, and deviated from i_1, i_2 due to the attitude error caused by gyro drift of FGU1 and FGU2.

(6) $\tilde{i}_0$: The coordinate systems coincided with i_0 at the initial time t_0, and deviated from i_0 due to the attitude error caused by gyro drift of FGU2.

III. THE Q-NNKF ALFORITHM FOR HULL DEFORMATION WITH LARGE MISALIGNMENT ANGLE

A. QUATERNION OPTIMIZATION METHOD

The function of quaternion optimization method, namely, method Q, is introduced to estimate most of the large misalignment angle φ_{02} [15]. After that, we can make linear approximation filtering estimation for the small residual hull deformation angle.

The result of quaternion optimization method, $C_{b_2}^{b_0}$, is the rotation matrix from b_2 to b_0, and its corresponding Euler angle vector is φ_{02}. The angular velocity of FGU1 and FGU2 are $\omega_1(t)$ and $\omega_2(t)$, respectively. Because the quaternion optimization method can estimate most of misalignment angle, the relationship of FGU1 and FGU2 is approximately expressed as:

$$\omega_1(t) = C_{b_2}^{b_0}(t) \cdot \omega_2(t) \tag{1}$$

Considering the hull deformation is a slow variety, $C_{b_2}^{b_0}(t)$ can be approximated to be a constant over a short period of time so that $C_{b_2}^{b_0}(t)$ can be denoted by $C_{b_2}^{b_0}$. By integrating on both side of the equation once, we get the following formula

$$\begin{aligned} \beta(t) &= C_{b_2}^{b_0} \cdot \alpha(t) \\ \beta(t) &= \int_0^t \omega_1(\tau) d\tau, \quad \alpha(\tau) = \int_0^t \omega_2(\tau)\, \mathrm{d}\tau \end{aligned} \tag{2}$$

Let $q = \begin{bmatrix} s & \eta \end{bmatrix}^T$ be the corresponding quaternion of $C_{b_2}^{b_1}$, so formula (2) can be expressed as

$$\beta(t) = q \otimes \alpha(t) \otimes q^* \tag{3}$$

Define the following operator:

$$\begin{bmatrix} + \\ q \end{bmatrix} = \begin{bmatrix} s & -\eta^T \\ \eta & sI + \eta(\times) \end{bmatrix}, \begin{bmatrix} - \\ q \end{bmatrix} = \begin{bmatrix} s & -\eta^T \\ \eta & sI - \eta(\times) \end{bmatrix} \tag{4}$$

The formula (2) can be transformed into the following linear equations in terms of q.

$$\left(\begin{bmatrix} + \\ \beta(t) \end{bmatrix} - \begin{bmatrix} - \\ \alpha(t) \end{bmatrix} \right) q = 0 \tag{5}$$

The optimum solution of q should satisfy the following formula

$$\begin{aligned} &\min_q \int_0^t \left\| \left(\begin{bmatrix} + \\ \beta(t) \end{bmatrix} - \begin{bmatrix} - \\ \alpha(t) \end{bmatrix} \right) q \right\|^2 dt = \min_q q^T K q \\ &K = \int_0^t \left(\begin{bmatrix} + \\ \beta(t) \end{bmatrix} - \begin{bmatrix} - \\ \alpha(t) \end{bmatrix} \right)^T \left(\begin{bmatrix} + \\ \beta(t) \end{bmatrix} - \begin{bmatrix} - \\ \alpha(t) \end{bmatrix} \right) \\ &\qquad dt, q^T q = 1 \end{aligned} \tag{6}$$

The Lagrange multiplier λ can be proposed in the following equation to solve these typical optimization problems:

$$L(q) = q^T K q - \lambda \left(q^T q - 1 \right) \tag{7}$$

By differentiating the formula (7) to q, we have

$$(K - \lambda I) q = 0 \tag{8}$$

The optimal quaternion q is the regularized eigenvector of K corresponding to the minimum eigenvalue λ.

$$L(q) = \lambda \tag{9}$$

The $C_{b_2}^{b_0}$ is the rotation matrix corresponding to the quaternion q. And φ_{02} is the Euler angle of $C_{b_2}^{b_0}$.

B. NEW ATTITUDE ANGLE MATCHING ALGORITHM FOR RESIDUAL SMALL ANGLE

According to the definition of coordinates, we can express the misalignment matrix between FGU1 and FGU2 as follow

$$C_{b_2}^{b_1} = C_{b_0}^{b_1} C_{b_2}^{b_0} \tag{10}$$

In (10), $C_{b_2}^{b_0}$ has been determined after the quaternion optimization method. And $C_{b_0}^{b_1}$ corresponds to the rest of whole misalignment angle which is small, it can be expressed as

$$C_{b_0}^{b_1} = C_{b_1}^{\tilde{i}_1 \, T} C_{\tilde{i}_1}^{i_1 \, T} C_{i_0}^{i_1} C_{\tilde{i}_0}^{i_0} C_{b_0}^{\tilde{i}_0} \tag{11}$$

According to the definition of coordinate system, $C_{b_0}^{\tilde{i}_0}$ can be written as

$$C_{b_0}^{\tilde{i}_0} = C_{i_0}^{\tilde{i}_0} C_{i_2}^{i_0} C_{\tilde{i}_2}^{i_2} C_{b_2}^{\tilde{i}_2} C_{b_0}^{b_2} \tag{12}$$

By substituting (12) into (11), we have

$$C_{i_2}^{\tilde{i}_2} C_{i_0}^{i_2} C_{i_1}^{i_0} C_{\tilde{i}_1}^{i_1} C_{b_1}^{\tilde{i}_1} C_{b_0}^{b_1} = C_{b_2}^{\tilde{i}_2} C_{b_0}^{b_2} \tag{13}$$

In (13), $C_{b_0}^{b_1}$ indicates the direction cosine matrix from b_0 frame to the FGU1 body coordinate frame b_1, and we will use the Kalman filter to estimate the value of $C_{b_0}^{b_1}$ in order to obtain the final result of $C_{b_2}^{b_1}$ which shows the whole deformation between FGU1 and FGU2. Let φ_{10} be Euler angle of $C_{b_0}^{b_1}$, and according to the definition of coordinate frame φ_{10} is small angle. So $C_{b_0}^{b_1}$ it can be written as

$$C_{b_0}^{b_1} \approx I + \begin{bmatrix} 0 & -\varphi_{10z} & \varphi_{10y} \\ -\varphi_{10z} & 0 & -\varphi_{10x} \\ \varphi_{10y} & -\varphi_{10x} & 0 \end{bmatrix} = I + [\varphi_{10}\times] \quad (14)$$

$C_{\tilde{i}_1}^{i_1}$ and $C_{\tilde{i}_2}^{i_2}$ are the attitude drift matrix of FGU1 and FGU2 which caused by gyro drift. Let $\theta_{1,i}$ and $\theta_{2,i}$ be the Euler angle of $C_{\tilde{i}_1}^{i_1}$ and $C_{\tilde{i}_2}^{i_2}$, if they are small angles, they can be described by

$$C_{\tilde{i}_1}^{i_1} \approx I + \left[\theta_{1,i}\times\right] \quad (15)$$

$$C_{\tilde{i}_2}^{i_2} \approx I + \left[\theta_{2,i}\times\right] \quad (16)$$

$C_{i_1}^{i_0}$ is the rotation matrix from FGU1 body coordinate frame b_1 to b_0 at the initial time t_0. Let φ_0 be the Euler angle of $C_{i_1}^{i_0}$, and according to the definition of coordinate system φ_0 is small angle, so $C_{i_1}^{i_0}$ is approximately expressed as

$$C_{i_1}^{i_0} \approx I - \begin{bmatrix} 0 & -\varphi_{0z} & \varphi_{0y} \\ -\varphi_{0z} & 0 & -\varphi_{0x} \\ \varphi_{0y} & -\varphi_{0x} & 0 \end{bmatrix} = I - [\varphi_0\times] \quad (17)$$

$C_{i_0}^{i_2}$ is the rotation matrix from i_0 to i_2, and at the initial time of t_0 it is same as $C_{b_0}^{b_2}$. Because $C_{i_0}^{i_2}$ is constant matrix, we have

$$C_{i_0}^{i_2} = C_{b_0}^{b_2} \quad (18)$$

From formulas (13)-(18), we have

$$\left\{I - \left[\theta_{2,i}\times\right]\right\} C_{b_0}^{b_2} \left\{I - [\varphi_0\times]\right\} \left\{I + \left[\theta_{1,i}\times\right]\right\} \times C_{b_1}^{\tilde{i}_1} \left\{I + [\varphi_{10}\times]\right\} = C_{b_2}^{\tilde{i}_2} C_{b_0}^{b_2} \quad (19)$$

On both sides of (19), let the formula be multiplied by $C_{b_2}^{b_0}$ on the left side and $C_{\tilde{i}_1}^{b_1}$ on the right side, respectively. After omitting the second-order small quantities, we get the formula as

$$\left\{I + \left[C_{b_1}^{\tilde{i}_1}\varphi_{10} + \theta_{1,i} - \varphi_0 - C_{b_2}^{b_0}\theta_{2,i}\right]\times\right\} = C_{b_2}^{b_0} C_{b_2}^{\tilde{i}_2} C_{b_0}^{b_2} C_{\tilde{i}_1}^{b_1} \quad (20)$$

In (20), $C_{b_1}^{\tilde{i}_1}$, $C_{b_2}^{\tilde{i}_2}$ are the attitude matrices of FGU1 and FGU2 calculated by the output of the FGUs, respectively. $C_{b_2}^{b_0}$ is calculated by quaternion optimization algorithm.

For the right side of the equation (20), let $C_{b_2}^{b_0} C_{b_2}^{\tilde{i}_2} C_{b_0}^{b_2} C_{\tilde{i}_1}^{b_1}$ be

$$C_{b_2}^{b_0} C_{b_2}^{\tilde{i}_2} C_{b_0}^{b_2} C_{\tilde{i}_1}^{b_1} = \begin{bmatrix} C_{11} & C_{12} & C_{13} \\ C_{21} & C_{22} & C_{23} \\ C_{31} & C_{32} & C_{33} \end{bmatrix} \quad (21)$$

Supposing $Z = \left[Z_x, Z_y, Z_z\right]^T$ is the Euler angle of $C_{b_2}^{b_0} C_{b_2}^{\tilde{i}_2} C_{b_0}^{b_2} C_{\tilde{i}_1}^{b_1}$, we have

$$Z_x = \arcsin\left(C_{32}\right)$$

$$Z_y = \arcsin\left(-\frac{C_{31}}{C_{33}}\right)$$

$$Z_z = \arcsin\left(-\frac{C_{12}}{C_{22}}\right) \quad (22)$$

According to (20) and (22), we get the measurement equation of hull deformation matching algorithm based on large misalignment:

$$Z = C_{b_1}^{\tilde{i}_1}\varphi_{10} + \theta_{1,i} - \varphi_0 - C_{b_2}^{b_0}\theta_{2,i} \quad (23)$$

where $\varphi_{10} = \left[\varphi_{10x}, \varphi_{10y}, \varphi_{10z}\right]^T$ is the Euler angle of $C_{b_0}^{b_1}$.

C. COMBINATION OF KALMAN FILTER AND NEURAL NETWORK

After obtaining the measurement equation of the small angle residual error φ_{10}, we need to carry out filtering calculation. Considering the further nonlinear approximate operation for small angle φ_{10}, we consider introducing combination of Kalman filter and neural network (NNKF) to achieve the purpose of accurate calculation.

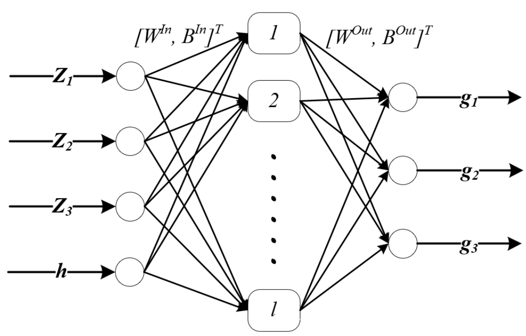

FIGURE 3. Typical multilayer neural network structure.

A two-layer parametric neural network and a nonlinear filtering algorithm are introduced to realize real-time estimation on line [21]. The two-layer parametric neural network contains four connection coefficients. They are input coefficient $\boldsymbol{W}^{In}$, input threshold b^{In}, output coefficient $\boldsymbol{W}^{Out}$, output threshold b^{Out} as shown in Fig. 3. The four vectors are combined as

$$\boldsymbol{Wb} = \left[\boldsymbol{W}^{In}\,\boldsymbol{b}^{In}\,\boldsymbol{W}^{Out}\,\boldsymbol{b}^{Out}\right]^T \quad (24)$$

In the small angle $\boldsymbol{\varphi}_{10}$, we can divide it into two categories according to the different frequencies. One kind which changes slowly is static deforming angle $\boldsymbol{\Phi}_{St}$, and the other kind which changes rapidly is dynamic deforming angle $\boldsymbol{\Phi}_{Dy}$.

$$\boldsymbol{\varphi}_{10} = \boldsymbol{\Phi}_{St} + \boldsymbol{\Phi}_{Dy} \quad (25)$$

Combining the connection weight coefficient vector and the variables in (23), we get the system state vector of nonlinear Kalman filter as

$$\boldsymbol{X} = \left[\boldsymbol{\Phi}_{St}\ \dot{\boldsymbol{\Phi}}_{St}\ \boldsymbol{\Phi}_{Dy}\ \dot{\boldsymbol{\Phi}}_{Dy}\ \boldsymbol{\theta}_{1,i}\ \boldsymbol{\theta}_{2,i}\ \boldsymbol{\varepsilon}_{c1}\ \boldsymbol{\varepsilon}_{c2}\ \boldsymbol{\varepsilon}_{r1}\ \boldsymbol{\varepsilon}_{r2}\ \boldsymbol{\varphi}_0\ \boldsymbol{Wb}\right]^T \quad (26)$$

For static deforming angle, considering to simulate the small amplitude deformation of hull deck in long-term voyage, we model it as quasi-static angular deformation:

$$\ddot{\boldsymbol{\Phi}}_{St} = \omega_{St} \tag{27}$$

where ω_{St} is the unit variance Gaussian white noise.

Dynamic deforming angle $\boldsymbol{\Phi}_{Dy}$ is set as a second-order Markov process as follows

$$\begin{aligned}\ddot{\Phi}_{Dy,i} + 2\mu_i \dot{\Phi}_{Dy,i} + b_i^2 \Phi_{Dy,i} = 2b_i\sqrt{D_i\mu_i}\omega_{Dy,i}(t), \\ i = x, y, z\end{aligned} \tag{28}$$

where μ_i is the dynamic deformation irregular coefficient, λ_i is the main frequency of dynamic deformation, D_i is the variance of dynamic deformation, w_{Dy} is the unit variance Gaussian white noise, and $b_i^2 = \mu_i^2 + \lambda_i^2$.

As Formulas (15) and (16) show, $\boldsymbol{\theta}_{1,i}$, $\boldsymbol{\theta}_{2,i}$ are the Euler angles of attitude errors caused by gyro drift. According to differential equation of direction cosine matrix, the state equations of $\boldsymbol{\theta}_{1,i}$, $\boldsymbol{\theta}_{2,i}$ can be expressed as

$$\begin{aligned}\theta_{1,i} &\approx -C_{b_1}^{\tilde{i}_1}(\varepsilon_{c1} + \varepsilon_{r1}) \\ \theta_{2,i} &\approx -C_{b_2}^{\tilde{i}_2}(\varepsilon_{c2} + \varepsilon_{r2})\end{aligned} \tag{29}$$

The random drift model of FOG is thought as first-order Markov process. And the constant drift of FGU is a constant. So we have the state equations of $\boldsymbol{\varepsilon}_{c1}$, $\boldsymbol{\varepsilon}_{c2}$, $\boldsymbol{\varepsilon}_{r1}$, $\boldsymbol{\varepsilon}_{r2}$ are

FOG1 constant drift: $\dot{\varepsilon}_{c1} = 0$

FOG1 random drift: $\dot{\varepsilon}_{c1} = 0$

$$\dot{\varepsilon}_{r1,i} = -\mu_{r1,i}\varepsilon_{r1,i} + \sigma_{r1,i}\sqrt{2\mu_{r1,i}}\omega_{r1,i}(t), \quad i = x, y, z$$

FOG2 constant drift: $\dot{\varepsilon}_{c2} = 0$

FOG2 random drift

$$\dot{\varepsilon}_{r2,i} = -\mu_{r2,i}\varepsilon_{r2,i} + \sigma_{r2,i}\sqrt{2\mu_{r2,i}}\omega_{r2,i}(t), \quad i = x, y, z$$

where $\mu_{r1,i}$, $\mu_{r2,i}$ are the first-order Markov coefficient of the gyro random drift of FOG1 and FOG2 in all three axial directions, respectively; $\sigma_{r1,i}$, $\sigma_{r2,i}$ are the gyro random drift mean square deviation of FOG1 and FOG2 in all three axial directions, respectively; $\omega_{r1,i}(t)$, $\omega_{r2,i}(t)$ are the white noise.

$\boldsymbol{\varphi}_0$ is the deformation angle at the initial time t_0, so it is a constant vector

$$\dot{\boldsymbol{\varphi}}_0 = 0 \tag{30}$$

In (26), let l be the number of neurons in the hidden layer, we have

$$\begin{aligned}\boldsymbol{W}^{In} &= \left[\left(W_1^{In}\right)^T, \left(W_2^{In}\right)^T, \left(W_3^{In}\right)^T\right]^T \\ \boldsymbol{b}^{In} &= \left[b_1^{In}, b_2^{In}, \cdots, b_l^{In}\right]^T \\ \boldsymbol{W}_i^{In} &= \left[W_{i,1}^{In}, W_{i,2}^{In}, \cdots, W_{i,l}^{In}\right]^T, \quad i = 1, 2, 3 \\ \boldsymbol{W}^{Out} &= \left[\left(W_1^{Out}\right)^T, \left(W_2^{Out}\right)^T, \cdots, \left(W_l^{Out}\right)^T\right]^T \\ \boldsymbol{b}^{Out} &= \left[b_1^{Out}, b_2^{Out}, b_3^{Out}\right]^T \\ \boldsymbol{W}_j^{Out} &= \left[W_{j,1}^{Out}, W_{j,2}^{Out}, W_{j,3}^{Out}\right]^T, \quad j = 1, 2, \cdots, l\end{aligned} \tag{31}$$

The weight coefficient of neural network can be regarded as slow variation, and it can be seen as a random walk process which finally converge to a value close to a constant. Therefore, we choose a model with a small random walk coefficient σ and white noise ω to describe the weight coefficient as follow

$$\begin{aligned}\dot{\boldsymbol{W}}^{In} &= \sigma_w^{In}\omega_w^{In} \\ \dot{\boldsymbol{b}}^{In} &= \sigma_b^{In}\omega_b^{r} \\ \dot{\boldsymbol{W}}^{Out} &= \sigma_w^{Out}\omega_w^{Out} \\ \dot{\boldsymbol{b}}^{Out} &= \sigma_b^{Out}\omega_b^{Out}\end{aligned} \tag{32}$$

According to the above equation, the system state equation can be written as

$$\hat{X}_{k+1} = f\left(\hat{X}_k\right) + \hat{G} \cdot \omega(k) \tag{33}$$

And the observation equation is

$$Z_{k+1} = h\left(\hat{X}_{k+1}\right) + g\left(Z_{k+1}, Wb_{k+1}\right) + v_{k+1} \tag{34}$$

where $h\left(\hat{X}_{k+1}\right) = \theta_{1i,k+1} - C_{b_2}^{b_0}\theta_{2i,k+1} - \varphi_{0,k+1}$, and v_{k+1} is the measurement noise. We write the neural network target output as $g(Z, Wb)$ where $\boldsymbol{Wb} = \left[W^{In}\, b^{In}\, W^{Out}\, b^{Out}\right]^T$, and the input is the observation vector $\boldsymbol{Z}$ in (22). Therefore, small deformation angle $\boldsymbol{\varphi}_{10}$ is estimated by $C_{\tilde{i}_1}^{b_1} g(Z, Wb)$. And the whole misalignment angle $\boldsymbol{\varphi}_{12}$ between FGU1 and FGU2 is

$$\boldsymbol{\varphi}_{12} = \boldsymbol{\varphi}_{10} + \boldsymbol{\varphi}_{02} \tag{35}$$

IV. EXPERIMENTAL RESULTS AND ANALYSIS

A. CONSTRUCTION OF EXPERIMENTAL ENVIRONMENT

In order to fully simulate the actual hull deformation on the ship, we use the physical experiment platform and computer simulation platform to form experiment environment as Fig. 4 shown. The hull deformation angle consists of static deformation angle and dynamic deformation angle. Static deformation angle is simulated by misalignment installation angle from physical platform and quasi-static deforming angle from computer simulation platform. Because the second-order Markov model is driven by white noise, dynamic deforming angle is generated by computer simulation platform. The turntable in physical platform is responsible for simulating the ship motion excitation. By the coordinate fusion operation, the original simulation data is obtained. After the simulation data of FGU1 and FGU2 is synchronized with time, the data enters the hull deformation test to verify validity and applicability of the algorithm.

As shown in Fig. 5, the physical experiment platform provides a high-precision turntable, two sets of FGUs, a data synchronous recording device, and a computer. The physical experiment platform can output the ship motion excitation,

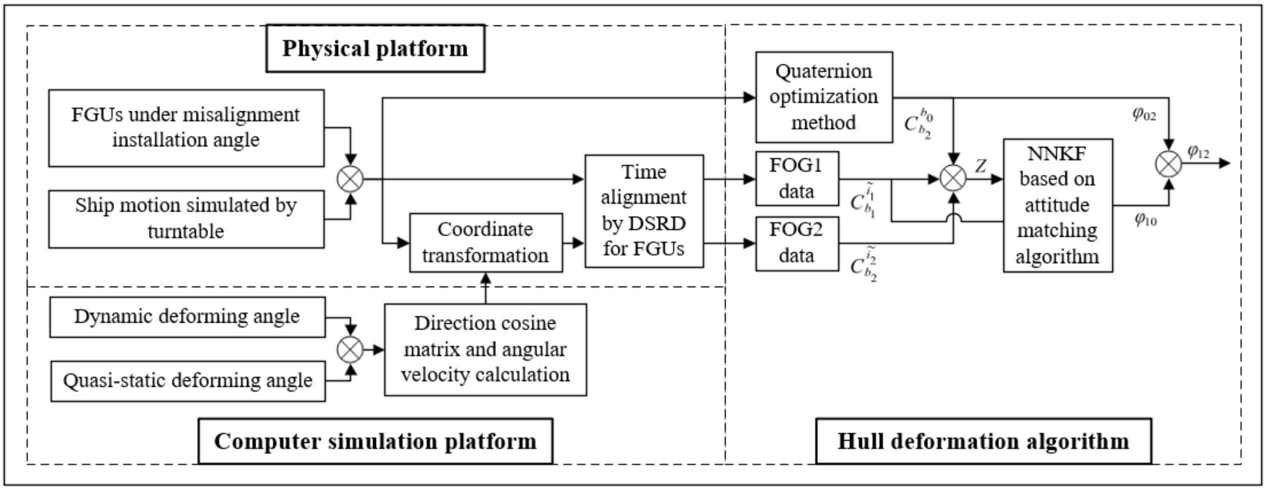

FIGURE 4. Experimental flow schematic diagram of hull deformation based on large misalignment angle.

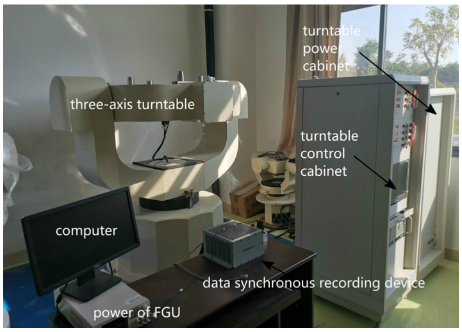

FIGURE 5. Physical simulation experiment platform of hull deformation based on large misalignment angle.

FGUs data, and be responsible for the time alignment of FGU1 and FGU2.

The high-precision turntable is responsible for simulating the motion of the hull, and the three axes are set as sinusoidal motion. The motion model is defined as follow

$$\begin{aligned} \psi &= \psi_p \sin\left(\omega_p t + \varphi_p\right) \\ \gamma &= \gamma_r \sin\left(\omega_r t + \varphi_r\right) \\ h &= h_y \sin\left(\omega_y t + \varphi_y\right) \end{aligned} \tag{36}$$

where $\psi_p = 3^\circ$, $\gamma_r = 4^\circ$, $h_y = 2^\circ$ are the amplitudes of vibrations on the axes of pitch, roll, yaw, and the sine period of three axes are 8s, 7s, 6s, respectively.

The two FGUs are fixedly installed in the inner loop of the high-precision turntable as shown in Fig. 6. In the inertial measurement unit systems, three fiber optic gyroscopes (FOG) are installed orthogonally. The random walk coefficient of each FOG is $0.003^\circ/\sqrt{\text{h}}$, and the bias stability is 0.005°/h (1σ). The outputs of FGUs are connected with data synchronous recording device (DSRD) through serial communication, and the sampling rate is set to 200 Hz.

Fig. 7 shows the DSRD. It contains data acquisition unit, serial port expansion circuit board and power module, and its responsibility is data acquisition and the time alignment of data. The data acquisition unit of DSRD is developed based on VXworks system and it supports synchronous acquisition and processing of multi-channel data. According to the FGU data time stamp, two sets of FGUs data are collected together,

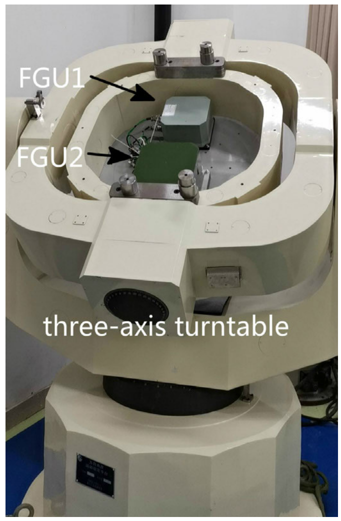

FIGURE 6. Two sets of FGUs fixedly installed with initial large misalignment angle.

FIGURE 7. Data synchronous recording device of hull deformation measurement system.

and the recording time error of the two sets of FGUs data is compressed within one sampling period, thus reducing the influence of the data time delay error of hull deformation calculation. The DSRD is connected with the computer through network communication to ensure the real-time and accuracy of FGU data recording.

The computer simulation platform is responsible for outputting quasi-static deforming angle and dynamic deforming angle in hull deformation. The quasi-static deforming angle is set as a sinusoidal motion with a period of 2 hours and an amplitude of 0.1° degrees to simulate the extremely slow change of the static deformation angle between FGU1 and FGU2 with time. And the dynamic deformation parameters of the three axes are set as shown in Table 1.

TABLE 1. Dynamic deformation simulation parameters setting.

Axes	Irregular coefficient, $\mu(1/s)$	Main frequency, $\lambda(Hz)$	Variance, $D(deg^2)$
X	0.15	0.20	4.5×10^{-7}
Y	0.10	0.15	2.1×10^{-7}
Z	0.08	0.10	1.6×10^{-7}

Finally, the measurement data from physical platform and the simulation data from computer simulation platform constitutes the simulation of hull deformation by coordinate transformation.

B. RESULT AND ANALYSIS OF METHOD Q

We use the quaternion optimization method (Method Q) to roughly estimate the most of misalignment angle φ_{02} between the two FGUs, in order to make preparation for the hull deformation filtering algorithm based on large misalignment angle. Therefore, our pursuing for this link is to quickly converge to obtain the results with certain accuracy.

In order to verify the performance of the quaternion optimization method, in this experiment, we set the initial large misalignment angle, i.e., the installation misalignment angle between the two FGUs as [250″; 1000″; 2400″], and other parameter settings remain unchanged, thus we can verify the convergence speed and accuracy of optimization quaternion for different estimation of small angle, medium angle and large angle.

In the hull deformation environment based on large misalignment angle, we respectively used the optimization quaternion method (OQ), the least squares estimation method (LSE) and the analytic coarse alignment method (ACA) to make preliminary estimate of the large misalignment angle. The quaternion optimization method and the least squares estimation method use only FOG data, the analytic coarse alignment method uses both FOG data and accelerometer data.

As shown in Figs. 8-10, in the environment of hull deformation based on the large misalignment angle, the convergence speed of OQ method is the fastest one in the three methods, which is about four times as fast as LSE method; the LSE method convergence speed takes second place with the general performance of convergence stability; ACA method has the worst convergence performance with an oscillating trend, which is not suitable for fast estimation of hull deformation based on large misalignment.

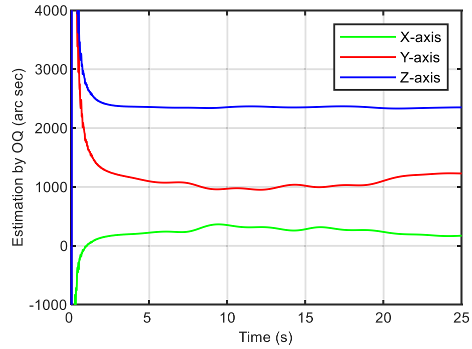

FIGURE 8. Estimation result of large misalignment angle by the optimization quaternion method (OQ).

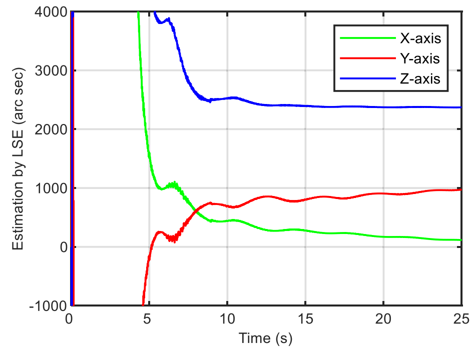

FIGURE 9. Estimation result of large misalignment angle by the least squares estimation method (LSE).

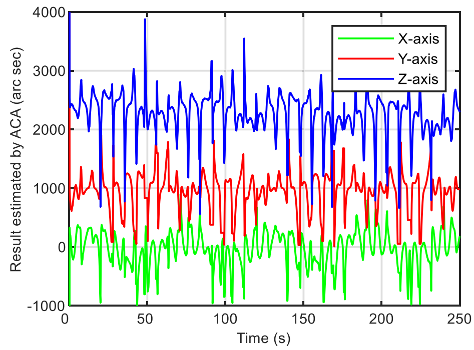

FIGURE 10. Estimation result of large misalignment angle by the analytic coarse alignment method (ACA).

Table. 2 shows the estimation results of large misalignment angle with the three methods after convergence stability, and we can conclude that OQ method have a relatively more accurate estimate of large alignment angle than the other two methods. Therefore, quaternion optimization method is a good choice to estimate the misalignment angle φ_{02} quickly with certain accuracy, and output of quaternion optimization

TABLE 2. Comparison of coarse registration result.

Axes	Optimization quaternion (arc sec)	Least squares estimation (arc sec)	Analytic course alignment method (arc sec)
X	266.1	197.5	170.8
Y	1060.5	880.4	991.9
Z	2352.4	2381.1	2306.1

method can meet the requirements of following hull deformation algorithm.

C. RESULT AND ANALYSIS OF Q-NNKF ALGORITHM

To estimate the whole misalignment angle φ_{12} of hull deformation, we use Q-NNKF to make more accurate calculation. In order to verify the validity of Q-NNKF method, we set the installation misalignment angle vector as [1.5°; 2°; 3°], and the other experimental parameters remain unchanged. In this link, we choose the traditional attitude angle matching algorithm with Conventional Kalman filter (CKF) and Extended Kalman Filter (EKF) for comparative experiments, respectively. Method CKF and Method EKF adopted the traditional attitude hull deformation matching measurement equation which didn't introduce the result of coarse registration:

$$Z = C_{\tilde{i}_1}^{b_1}(\theta_i^1 - \theta_i^2 - \varphi_0) + \varphi \tag{37}$$

where Z is the Euler angle of $C_{b_1}^{\tilde{i}_1\,T} C_{b_2}^{\tilde{i}_2}$.

To make sure that the comparison between the proposed method and the comparative method is fair, the experimental environment and the original parameters are completely consistent among the different test.

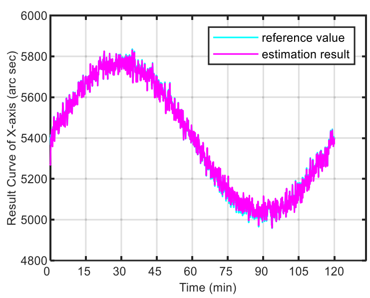

FIGURE 11. Hull deformation estimation result of Q-NNKF on X-axis.

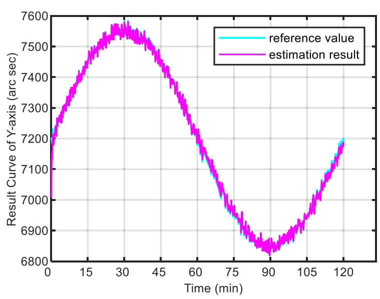

FIGURE 12. Hull deformation estimation result of Q-NNKF on Y-axis.

Figs. 11-13 show that the performance of algorithm estimation result and the reference value of Q-NNKF. We can see that the Q-NNKF has a good tracking effect on the hull deformation under the condition of large misalignment angle.

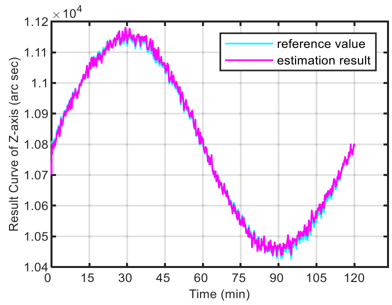

FIGURE 13. Hull deformation estimation result of Q-NNKF on Z-axis.

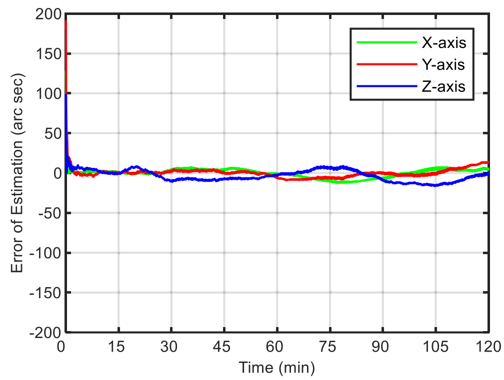

FIGURE 14. Error of estimation of Q-NNKF on three axes.

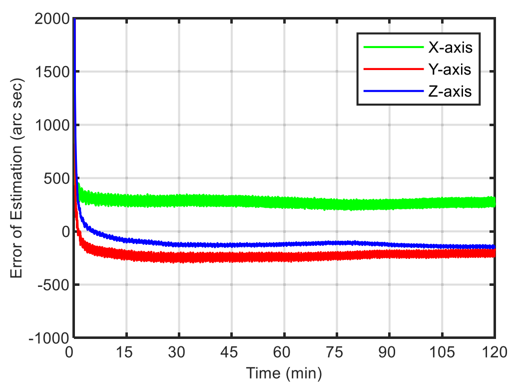

FIGURE 15. Error of estimation of CKF on three axes.

Fig. 14 shows the estimation error of Q-NNKF method, and the root mean square error (RMSE) vector on three axes is [5.1909″; 4.4826″; 7.6578″]. At the same time, Fig.15 shows the estimation error of Method CKF, and the RMSE of Method CKF is [280.0055″; 226.2037″; 122.5661″]; Fig.16 shows the estimation error of Method EKF and the RMSE of Method EKF is [274.2886″; 220.7788″; 109.0031″]. Therefore, compared with CKF and EKF, we can find that the hull deformation filtering algorithm for the large misalignment proposed in this paper can effectively reduce the estimation error of hull deformation with large misalignment angle.

TABLE 3. RMSE of method CKF results under different misalignment angle.

Misalignment angle (deg)	0	0.5	1	1.5	2	2.5	3	3.5	4	4.5
X-axis (arc sec)	4.163	13.682	47.401	108.254	195.637	305.509	444.259	611.157	803.820	1027.010
Y-axis (arc sec)	3.051	17.913	53.928	119.032	201.161	309.073	440.709	592.107	759.474	946.302
Z-axis (arc sec)	2.811	9.759	33.462	65.966	116.614	167.941	236.756	315.326	401.871	500.301

TABLE 4. RMSE of method EKF results under different misalignment angle.

Misalignment angle (deg)	0	0.5	1	1.5	2	2.5	3	3.5	4	4.5
X-axis (arc sec)	3.678	13.804	52.136	116.165	202.691	312.205	456.675	623.647	821.257	1046.251
Y-axis (arc sec)	2.961	9.683	45.231	102.717	188.211	293.038	415.090	561.548	728.516	912.244
Z-axis (arc sec)	3.968	8.781	26.203	57.348	96.882	146.314	206.332	286.420	365.081	457.5889

TABLE 5. RMSE of method NNKF results under different misalignment angle.

Misalignment angle (deg)	0	0.5	1	1.5	2	2.5	3	3.5	4	4.5
X-axis (arc sec)	2.222	10.603	39.611	82.958	146.793	234.571	321.243	444.555	621.694	803.267
Y-axis (arc sec)	4.367	10.499	28.070	69.130	119.276	168.116	215.790	328.036	346.979	387.452
Z-axis (arc sec)	4.769	11.904	40.176	83.304	128.54	196.758	275.798	394.444	414.503	468.863

TABLE 6. RMSE of method Q-NNKF results under different misalignment angle.

Misalignment angle (deg)	0	0.5	1	1.5	2	2.5	3	3.5	4	4.5
X-axis (arc sec)	2.647	1.485	2.146	4.568	1.648	4.499	1.230	3.065	1.692	2.863
Y-axis (arc sec)	2.685	3.784	2.993	4.258	3.095	2.321	2.707	3.268	2.370	4.989
Z-axis (arc sec)	5.935	2.763	1.636	3.908	4.836	2.621	5.836	1.564	5.995	4.573

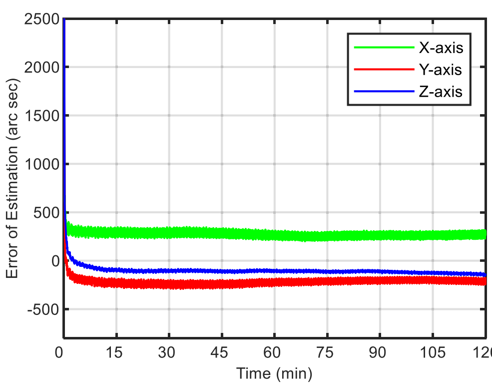

FIGURE 16. Error of estimation of EKF on three axes.

To furtherly analyze the effect of different large misalignment angles on the hull deformation matching algorithm, and verify the applicability of the Q-NNKF algorithm proposed in this paper, we carried out more tests.

We set ten groups of experiments, and in each group of experiments the large misalignment angles on three axial directions are the same. The large misalignment angles in ten groups of experiments were set as 0°, 0.5°, 1°, 1.5°, 2°, 2.5°, 3°, 3.5°, 4°, 4.5°, respectively. We choose the results of four methods for comparison, including Method CKF, Method EKF, traditional attitude angle matching algorithm with Kalman filtering with neural network (NNKF), the method proposed in this paper (Q-NNKF). Method CKF adopted conventional Kalman filtering without coarse registration process; Method EKF adopted Extended Kalman filtering without coarse registration process; Method NNKF adopted Kalman filtering with neural network; Q-NNKF adopted the brand-new attitude angle matching algorithm combined with NNKF filter as introduced in this paper.

Tables 3-6 respectively show the RMSE of Method CKF, Method EKF, Method NNKF, and Method Q-NNKF with the increase of the large installation misalignment angle. From the four tables, we can get that when the large installation misalignment angle between FGU1 and FGU2 is relatively small, the accuracy of the four methods is similar. With the increment of the large installation misalignment angle, the nonlinear factors in the system measurement model become larger, and the accuracy of the contrast algorithms is affected to varying degrees

In order to more intuitively analyze the effect of large misalignment angle on the accuracy of hull deformation algorithm, RMSE curves of the four methods results on three axes with the changes of the large misalignment angle are respectively plotted in the Figs. 17-19.

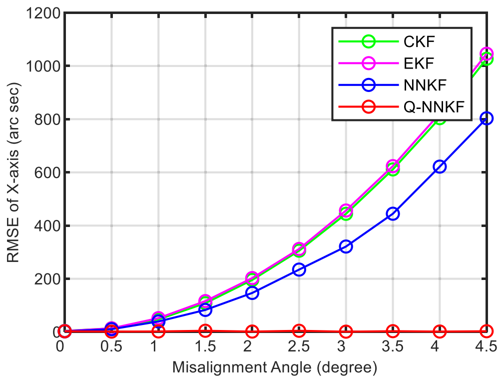

FIGURE 17. RMSEs of CKF, EKF, NNKF, Q-NNKF on X-axis.

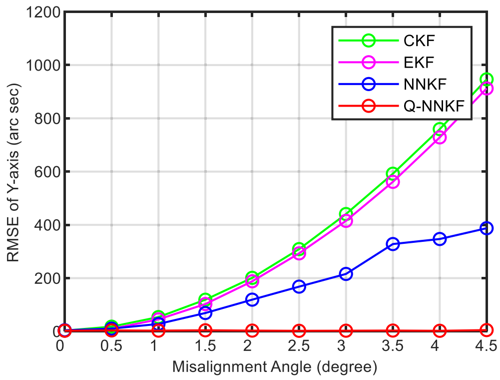

FIGURE 18. RMSEs of CKF, EKF, NNKF, Q-NNKF on Y-axis.

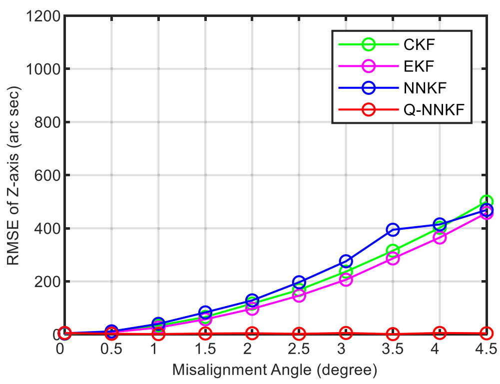

FIGURE 19. RMSEs of CKF, EKF, NNKF, Q-NNKF on Z-axis.

The accuracy of Method CKF is greatly affected by the increase of misalignment angle, and the error of Method CKF begins to increase exponentially from less than 10″ to hundreds of arcseconds.

The accuracy of Method EKF is slightly better than Method CKF in the calculation of hull deformation with large misalignment angle. Because the performance of EKF algorithm depends on the local nonlinearity of the model, and the high-order terms ignored in the linearization process will affect the accuracy of the results, the results of Method CKF in calculating hull deformation under large misalignment angle are not satisfactory.

Method NNKF combines the linear approximation characteristic of neural network, it performed better than CKF and EKF in dealing with the model nonlinearity caused by large misalignment angle. However, due to the lack of coarse registration process, the accuracy of NNKF is still greatly affected by large misalignment angle.

Method Q-NNKF obtains the coarse registration result of hull deformation by using quaternion optimization method, and substitutes the result into the attitude angle matching algorithm proposed in this paper to obtain the measurement equation to estimate the residual part of hull deformation misalignment angle, which can effectively reduce the nonlinearity of the measurement equation model. Then, the neural network Karman filter is used for filtering operation, and the nonlinear error of the whole algorithm is further reduced by the linear approximation characteristic of neural network. From fig. 17-fig. 19 and Table 6, we can see that the accuracy of Q-NNKF is relatively high, and it is almost not affected by large misalignment angle.

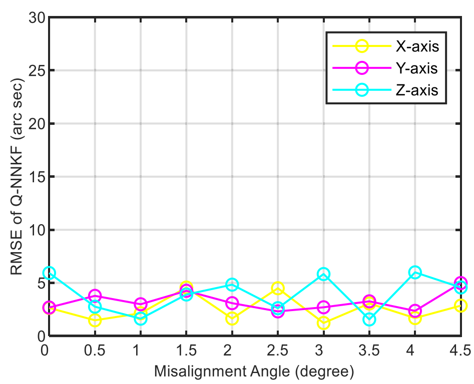

FIGURE 20. RMSEs of Q-NNKF under different misalignment angles.

As shown in Fig. 20, RMSE of Q-NNKF algorithm results are all less than 10″ under the condition of large misalignment angle, even if the installation misalignment angle increases from 0° to 4.5°. RMSE of Q-NNKF algorithm results no longer change with the size of large misalignment angle. The experiment results show that Q-NNKF method can accurately estimate hull deformation under the condition of large misalignment angle.

V. CONCLUSION

In this paper, we present a real-time hull deformation measurement algorithm, namely, Q-NNKF, and apply the algorithm to hull deformation measurement with large misalignment angle to solve the nonlinear error problem. By optimizing the coarse registration result parameters estimated by Method Q, we deduced a brand-new attitude angle matching algorithm to reduce the nonlinear error caused by large misalignment angle. After that, NNKF was utilized to perform filtering calculation to make a further nonlinear approximation filter for the residual part of the large misalignment angle. The field test experiments show that the proposed algorithm can accurately calculate hull deformation with large misalignment angle, and the RMSE of method is less than $10''$.

In the future work, we should consider the hull deformation matching algorithm under the condition of time-varying large misalignment angle, rather than the fixed large initial installation misalignment angle.

REFERENCES

[1] S. Minakuchi, T. Sanada, N. Takeda, S. Mitani, T. Mizutani, Y. Sasaki, and K. Shinozaki, ''Thermal strain in lightweight composite fiber-optic gyroscope for space application,'' *J. Lightw. Technol.*, vol. 33, no. 12, pp. 2658–2662, Jun. 15, 2015.

[2] K. Li, L. Chang, and Y. Chen, ''Common frame based unscented quaternion estimator for inertial-integrated navigation,'' *IEEE/ASME Trans. Mechatronics*, vol. 23, no. 5, pp. 2413–2423, Oct. 2018.

[3] L. Chang, Y. Li, and B. Xue, ''Initial alignment for a Doppler velocity log-aided strapdown inertial navigation system with limited information,'' *IEEE/ASME Trans. Mechatronics*, vol. 22, no. 1, pp. 329–338, Feb. 2017.

[4] X. Wang, ''Fast alignment and calibration algorithms for inertial navigation system,'' *Aerosp. Sci. Technol.*, vol. 13, nos. 4–5, pp. 204–209, Jun. 2009.

[5] J. Wang, T. Zhang, B. Jin, Y. Zhu, and J. Tong, ''Student's t-based robust Kalman filter for a SINS/USBL integration navigation strategy,'' *IEEE Sensors J.*, vol. 20, no. 10, pp. 5540–5553, May 2020.

[6] Y. Wang, F. Sun, Y. Zhang, H. Liu, and H. Min, ''Central difference particle filter applied to transfer alignment for SINS on missiles,'' *IEEE Trans. Aerosp. Electron. Syst.*, vol. 48, no. 1, pp. 375–387, Jan. 2012.

[7] P. M. G. Silson, ''Coarse alignment of a ship's strapdown inertial attitude reference system using velocity loci,'' *IEEE Trans. Instrum. Meas.*, vol. 60, no. 6, pp. 1930–1941, Jun. 2011.

[8] Z. F. Syed, P. Aggarwal, X. Niu, and N. El-Sheimy, ''Civilian vehicle navigation: Required alignment of the inertial sensors for acceptable navigation accuracies,'' *IEEE Trans. Veh. Technol.*, vol. 57, no. 6, pp. 3402–3412, Nov. 2008.

[9] A. V. Mochalov and A. V. Kazantsev, ''Use of ring laser units for measurement of moving object deformations,'' in *Proc. 2nd Int. Conf. Lasers for Meas. Inf. Transf.*, Saint Petersburg, Russia, Feb. 2002, pp. 85–92.

[10] W. Wu, S. Chen, and S. Qin, ''Online estimation of ship dynamic flexure model parameters for transfer alignment,'' *IEEE Trans. Control Syst. Technol.*, vol. 21, no. 5, pp. 1666–1678, Sep. 2013.

[11] H. Dai, J. Lu, W. Guo, G. Wu, and X. Wu, ''IMU based deformation estimation about the deck of large ship,'' *Optik*, vol. 127, no. 7, pp. 3535–3540, Apr. 2016.

[12] W. Yanyan, Z. Ya, W. Kai, W. Zhuo, C. Jiachong, and X. Dingjie, ''Research on multi-model adaptive hull deformation measurement algorithm,'' in *Proc. IEEE/ION Position, Location Navigat. Symp. (PLANS)*, Portland, OR, USA, Apr. 2020, pp. 718–722.

[13] J. Li, J. Fang, and M. Du, ''Error analysis and gyro-bias calibration of analytic coarse alignment for airborne POS,'' *IEEE Trans. Instrum. Meas.*, vol. 61, no. 11, pp. 3058–3064, Nov. 2012.

[14] Y. Huang, Y. Zhang, and X. Wang, ''Kalman-filtering-based in-motion coarse alignment for odometer-aided SINS,'' *IEEE Trans. Instrum. Meas.*, vol. 66, no. 12, pp. 346–354, Dec. 2017.

[15] J. Lu, L. Xie, and B. Li, ''Applied quaternion optimization method in transfer alignment for airborne AHRS under large misalignment angle,'' *IEEE Trans. Instrum. Meas.*, vol. 65, no. 2, pp. 346–354, Feb. 2016.

[16] K. Nam, S. Oh, H. Fujimoto, and Y. Hori, ''Estimation of sideslip and roll angles of electric vehicles using lateral tire force sensors through RLS and Kalman filter approaches,'' *IEEE Trans. Ind. Electron.*, vol. 60, no. 3, pp. 988–1000, Mar. 2013.

[17] F. Jiancheng and Y. Sheng, ''Study on innovation adaptive EKF for in-flight alignment of airborne POS,'' *IEEE Trans. Instrum. Meas.*, vol. 60, no. 4, pp. 1378–1388, Apr. 2011.

[18] G. Wei, S. Wei, X. Bo, and D. L. Ying, ''Nonlinear deformation measurement method based on IMU for ship,'' in *Proc. IEEE Int. Conf. Mechatronics Automat. (ICMA)*, Beijing, China, Aug. 2015, pp. 1397–1401.

[19] K. A. Kramer, S. C. Stubberud, and J. A. Geremia, ''Target registration correction using the neural extended Kalman filter,'' *IEEE Trans. Instrum. Meas.*, vol. 59, no. 7, pp. 1964–1971, Jul. 2010.

[20] R. Bisoi and P. K. Dash, ''A hybrid evolutionary dynamic neural network for stock market trend analysis and prediction using unscented Kalman filter,'' *Appl. Soft Comput.*, vol. 19, pp. 41–56, Jun. 2014.

[21] Y. He, X. Zhang, and X. Peng, ''A model-free hull deformation measurement method based on attitude quaternion matching,'' *IEEE Access*, vol. 6, pp. 8864–8869, Feb. 2018.

DONGSHENG XU received the B.S. degree from the College of Information Science and Engineering, Northeastern University, Liaoning, China, in 2016. He is currently pursuing the Ph.D. degree with the School of Aerospace Engineering, Xiamen University. His current research interests include inertial navigation, integrated navigation, and filtering algorithm.

XIAFU PENG received the M.S. degree in control theory and applications from the Harbin Institute of Naval Engineering, Harbin, China, and the Ph.D. degree in control science and engineering from Harbin Engineering University, Harbin, in 2001. Since 2002, he has been with the Department of Automation, Xiamen University, China, where he is currently a Professor. His research interests include inertial technology and intelligent transportation systems.

XIAOLI ZHANG received the Ph.D. degree in control theory and application from Northeastern University, China. From 2002 to 2003, he was a Postdoctoral Research Fellow with the Department of Automation, Tsinghua University. Since 2004, he has been with the Department of Automation, Xiamen University, China, where he is currently an Associate Professor. His main research interests include inertial technology and integrated navigation systems.

GONGLIU YANG received the Ph.D. degree in precision instrumentation and mechanism from Tsinghua University, Beijing, China, in 2004. He is currently a Professor with the School of Instrumentation and Optoelectronic Engineering, Beihang University. His current research interests include inertial navigation and integrated navigation.

XIAOQIANG HU received the B.S. degree from the School of Information Science and Technology, Xiamen University, Fujian, China, and the M.S. degree from the School of Aeronautics and Astronautics, Xiamen University. He is currently pursuing the Ph.D. degree with the Department of Automation, Xiamen University, Xiamen. His research interests include robotics, integrated navigation, and fault diagnosis.